IEEE International Conference on Robotics and Automation
San Diego, California, 1994

Estimation of Environment Forces and Rigid-Body Velocities using Observers

P. J. Hacksel and S. E. Salcudean
Department of Electrical Engineering
University of British Columbia
Vancouver, BC, V6T 1Z4, Canada

Abstract

This paper presents an observer-based approach to the determination of environment forces acting on a rigid body. Actuation forces, measured positions and orientations and identification of inertial parameters are used for this purpose.
It is also shown that environment force estimates can be used in turn to correct rigid-body velocity estimates generated by observers, leading to accurate, low-noise estimates during contact tasks. The approach, shown to also apply to general serial mechanisms, is supported by experimental data obtained with a magnetically levitated wrist.
0

1 Introduction

The use of linearized-model, observer-based control is a standard practice for plants with known and time-invariant dynamics. Its advantages are that the state estimates are obtained without the use of expensive sensors and lead to less noisy estimates than can be obtained by direct differentiation.

In the area of robotics, observers can be used to obtain improved position tracking control of manipulators, by providing accurate joint velocity estimates without the use of tachometers. A nonlinear model-based joint rate observer for serial kinematic mechanisms has been presented in [1]. In [2], a model-based observer was used with sliding-mode control of a robot to show good position trajectory tracking. Motivated by the need to accurately control a magnetically levitated (maglev) wrist for precision assembly [3, 4], for active vibration control [5], and teleoperation [6], a model-based approach was also used in [7] to design an angular-velocity observer for rigid body motion.

In order to produce small errors, the rigid-body motion velocity observers developed so far require accurate plant models. This includes small errors in the mass parameters and the absence of unmodelled dynamics and environment forces and torques. In the case of direct-drive robots, the plant model can be very accurate, provided that the robot mass parameters are identified [8].

In this paper, it is shown how model-based observers can be used to accurately estimate the environment forces acting on a rigid body. Furthermore, it is shown how these force estimates can be used to correct the observer-based velocity estimates of a rigid body. This implies that, given an accurate robot model, accurate environment force estimates and accurate velocity estimates can both be determined without the need for sensors or signal differentiation. Experimental results with the University of British Columbia (UBC) maglev wrist [6] support the analysis and are also presented in this paper.

The paper is organized as follows: Section 2 shows how environment forces acting on a rigid body can be estimated from observers, Section 3 describes two methods for correcting observer velocity estimates in the presence of unknown environment forces, and Section 4 presents an extension to serial mechanisms using the results in [1]. Experimental results with the UBC maglev wrist are presented in Section 5 and conclusions are presented in Section 6.

2 Observer-based Force Estimation

This section describes an observer-based method of estimating environment forces and torques acting on a controlled rigid body from measurements of its position and orientation and knowledge of the control forces and torques. The essential idea is to consider the observer error dynamics as a damped spring-mass system driven by the environment force (torque). By choosing sufficiently large gains to simulate a stiff spring, then measuring the displacement of the spring from its equilibrium, a good estimate of the environment force (torque) can be made.

Estimating environment forces from observer errors is similar to measuring forces from the position error of a PD-controlled rigid body. However, PD-error-based estimates depend on the controller gains, which are usually chosen to suit a specific task, and not to provide a force measurement. The advantage of observer based estimation is that the observer gains may be set independently of the controller gains. Control strategies other than PD control can also be used without any effect on observer estimate quality

The observer based estimation scheme is illustrated in Figure 1.

2.1 Linear Force Estimator

A simple state observer for a rigid body of mass m obeying Newton's law, $m\ddot{x} = m\dot{v} = f$, takes the form:

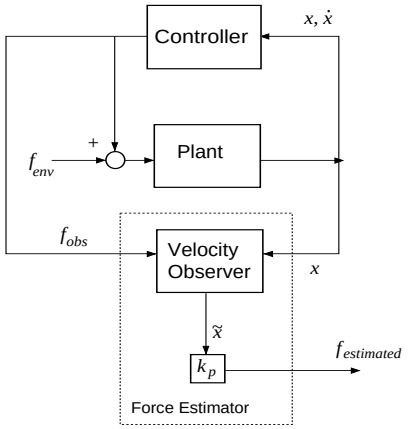

Figure 1: Force Estimator: The error $\tilde{x}$ is equivalent to the true environment force, f_{env}, passed through the filter $\frac{1}{ms^2+k_v s+k_p}$. $f_{estimated}$ is the estimated environment force.

$$\begin{aligned} \dot{\hat{v}} &= \frac{f}{m} + \frac{k_p}{m}(x-\hat{x}) = \frac{f}{m} + \frac{k_p}{m}\tilde{x} \\ \dot{\hat{x}} &= \hat{v} + \frac{k_v}{m}\tilde{x} \end{aligned} \tag{1}$$

where $\hat{x}$ and $\hat{v}$ are the observer values for the position x and velocity v and k_p, k_v are positive constants. It is assumed that the total force $f = f_{obs} + f_{env}$ applied to the plant is the sum of a known control force f_{obs} fed to the observer and an unknown environment force f_{env}. Subtracting the observer equations (1) from Newton's law results in the following error dynamics:

$$\begin{aligned} m\dot{\tilde{v}} &= f_{env} - k_p\tilde{x} \\ \dot{\tilde{x}} &= \tilde{v} - \frac{k_v}{m}\tilde{x}\ , \end{aligned} \tag{2}$$

where $\tilde{v} = v - \hat{v}$. Eliminating $\tilde{v}$ and $\dot{\tilde{v}}$ in (2) gives:

$$f_{env} = k_p\tilde{x} + k_v\dot{\tilde{x}} + m\ddot{\tilde{x}} \tag{3}$$

i.e., the dynamics for a mass attached to a damped spring driven by the environment force.

For a constant environment force f_{env} the differential equations (2) are stationary for

$$\begin{aligned} \tilde{x} &= \bar{x} \equiv \frac{1}{k_p}f_{env} \\ \tilde{v} &= \bar{v} \equiv \frac{k_v}{m}\tilde{x} = \frac{k_v}{mk_p}f_{env}\,. \end{aligned} \tag{4}$$

Note that at equilibrium, the observed error $\tilde{v}$ is directly proportional to $\tilde{x}$.

The deflection of the equilibrium reflects a stretching of an imaginary spring loaded by the environment force. Hence at low frequencies, *a good estimate of the force can be obtained as* $f_{env} = k_p\tilde{x}$.

There is a practical limit to the chosen magnitudes of k_p and k_v. To be accurately measured, forces must be large enough to create a deflection above the noise level of the position measurements. A very stiff, heavily damped spring would not deflect significantly for small forces, and would therefore require very high resolution position sensing. Thus there is a tradeoff involved in choosing appropriate gains; they must be chosen large enough to ensure reasonable behavior of the observer within the desired bandwidth, and small enough that the signal to noise ratio of the force measurement is sufficiently high.

2.2 Nonlinear Torque Estimator

The orientation dynamics of a rigid body are nonlinear and are given by

$$\frac{d}{dt}(J\omega) = \tau \tag{5}$$

$$\frac{d}{dt}\begin{bmatrix}\beta_o\\ \beta\end{bmatrix} = \frac{1}{2}\begin{bmatrix}-\beta^T\\ \beta_o I - (\beta\times)\end{bmatrix}\omega\ , \tag{6}$$

where J_0 is the inertia matrix in body frame, Q is the direction cosine matrix of a body frame relative to an inertial frame, $J = QJ_0Q^T$, ω is the angular velocity of the body, and β_o and β are the scalar and vector part of the Euler quarternion corresponding to Q [7].

Euler quarternions are a minimal nonsingular representation of orientation and can be used to construct an angular velocity observer [7], given by

$$\frac{d}{dt}(J\hat{\omega}) = \tau + \frac{1}{2}k_pJ^{-1}\mathbf{e}sgn(e_o) \tag{7}$$

$$\frac{d}{dt}\begin{bmatrix}\hat{\beta}_o\\ \hat{\beta}\end{bmatrix} = \frac{1}{2}\begin{bmatrix}-\hat{\beta}^T\\ \hat{\beta}_o I + \left(\hat{\beta}\times\right)\end{bmatrix}Q^T\left(\hat{\omega} + k_vJ^{-1}\mathbf{e}sgn(e_o)\right) \tag{8}$$

where e_o and $\mathbf{e}$ form the quarternion representation of the attitude error between the actual body and the observed body frames [7].

This observer was designed using the second order linear velocity observer (1) as an analogue and was shown to provide asymptotically correct estimates. As in the linear case, an estimate of the environment torque can be obtained by monitoring the difference in orientation between the actual body and observed body. While linear concepts, such as frequency response, do not have any meaning in the nonlinear case, we can expect a similar behavior to the linear case. With an environment torque τ_{env} , the error equations for the observer (7) become:

$$\begin{aligned} \dot{\mu} &= \tau_{env} - \frac{1}{2}k_pJ^{-1}\mathbf{e}\,sgn(e_o) \\ \dot{e}_o &= -\frac{1}{2}\mathbf{e}^TJ^{-1}(\mu - k_v\mathbf{e}sgn(e_o)) \\ \dot{\mathbf{e}} &= \frac{1}{2}[e_oI - (\mathbf{e}\times)]J^{-1}(\mu - k_v\mathbf{e}sgn(e_o))\ , \end{aligned} \tag{9}$$

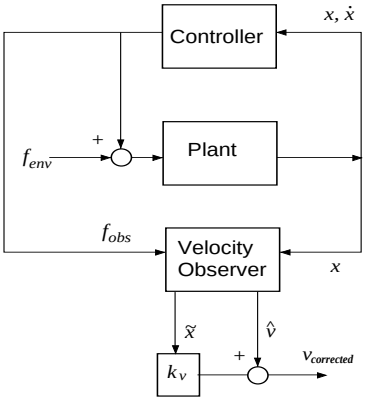

Figure 2: Correcting a Velocity Observer With Output Term: The velocity output is corrected by adding a multiple of the error $\tilde{x}$.

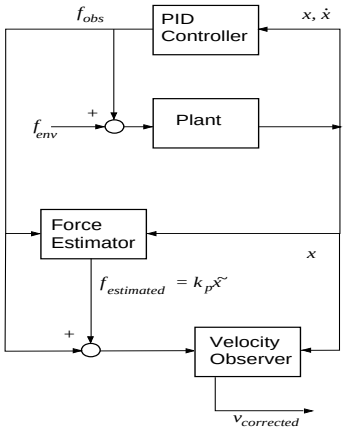

Figure 3: Correcting a Velocity Observer With a Force Estimator: The velocity observer input is corrected to include the force estimate.

where $\mu = J(\omega - \hat{\omega})$. The differential equations (9), are stationary for:

$$\begin{aligned} \mathbf{e} &= \bar{\mathbf{e}} \equiv \frac{2}{k_p} J \tau_{env} \qquad (10) \\ \mu &= \bar{\mu} \equiv k_v \bar{\mathbf{e}} = \frac{2k_v}{k_p} J \tau_{env} \\ e_o &= \bar{e}_o = \sqrt{1 - \mathbf{e}^T \mathbf{e}} \ . \end{aligned}$$

It is easily shown that $sgn\,(\bar{e}_o) = 1$. It is important to note that, unless the body has the inertia of a uniform sphere, (9) is not stationary for a constant environment torque τ_{env}, since J varies with time. However, simulations and experimental results show that the behaviour of the torque estimator still resembles that of the force estimator [9]. Hence, at low frequencies, *a good estimate of the environment torque can be obtained as* $\tau_{env} = (k_p/2)J^{-1}\mathbf{e}$.

The quality of the torque estimator can be expected to deteriorate if torques are large enough to create large error angles, as the nonlinearity of the system becomes more apparent. In fact, since the error term is described by a normalized quarternion, the maximum torque that can be allowed in (9) is bounded by $\left\|(k_p/2)J_0^{-1}\right\|$. A practical limit on the torque should be somewhat smaller, particularly when the torque input has high bandwidth, to allow for tracking errors.

3 Velocity Observation

For observer-based control of manipulators, accurate dynamic models and the absence of environment forces are required. It will now be shown that the force observer described in Section 2 may be used to correct the estimates of a velocity observer, so that it might be used for control purposes. As will be shown later, without some correction, velocity observation is almost useless in the presence of significant environment forces. Two ways of correcting observed velocities will be shown next.

3.1 Output Position Error Correction

Equations (4) and (10) describe the stationary behavior of the linear and angular velocity observers under a constant force or torque. Therefore, after an initial transient has subsided, the velocity estimate in (1) in the presence of an unknown but constant force can be corrected as follows:

$$v_{corrected} = \hat{v} + \bar{v} = \hat{v} + \frac{k_v}{m}\tilde{x} = \dot{\hat{x}} \, . \qquad (11)$$

Assuming that the angular velocity observer has a similar dynamic behaviour, the angular velocity estimate in (7) can be corrected as follows:

$$\begin{aligned} \mu_{corrected} &= \mu + \bar{\mu} = \mu + k_v \mathbf{e} \qquad (12) \\ \omega_{corrected} &= \hat{\omega} + k_v J^{-1} \mathbf{e} = \hat{\Omega} \, , \end{aligned}$$

where $\hat{\Omega}$ is the angular velocity corresponding to the observer quaternion $\hat{\beta}_0, \hat{\beta}$. A block diagram representing this approach is given in Figure 2.

The simplicity of the correction is devalued by the fact that $\dot{\hat{x}}$ and $\hat{\Omega}$, as estimates of velocity and angular velocity, are prone to higher levels of noise. Indeed, only one integration of the applied force is used to obtain $\dot{\hat{x}}$ and $\hat{\Omega}$, whereas obtaining $\hat{v}$ and $\hat{\omega}$ requires integrating twice.

3.2 Input Force Estimate Correction

Assuming a perfect model, the rigid-body velocity estimated by an observer can be corrected by adding measured environment forces (torques) to the observer input. If such measurements are not available, estimates as described in Section 2 can be employed instead. A block diagram of a control scheme employing such force estimates is shown in Figure 3. The control scheme involves the use of two observers. One performs the usual function of velocity estimation, while the other, with faster time constants, is used to estimate environment forces (torques). Since the sum of

the control and environment forces are added to the velocity observer input, the low frequency components of the velocity error can be removed without increasing the noise content of the observer estimate.

4 Extension to Serial Mechanisms

The force/torque observation technique outlined above can also be applied to general serial link mechanisms. An observer for such mechanisms was developed by Nicosia *et. al* [1]. The observer used here is a simplified version of the Nicosia observer, and is designed to handle a general robot model

$$D(q)\ddot{q} + C(q,\dot{q})\dot{q} + G(q) = u \tag{13}$$

described in generalized coordinates q, with $C(q,\dot{q})$ in Cristoffel form, and is given by

$$\begin{aligned} \dot{\hat{x}}_1 &= \hat{x}_2 + k_v\tilde{x}_1 \qquad (14)\\ \dot{\hat{x}}_2 &= D^{-1}(q)\left(-C\left(q,\dot{\hat{x}}_1\right)\dot{\hat{x}}_1 - G(q) + K_p\tilde{x}_1 + u\right)\\ \tilde{x}_1 &= q - x_1\ . \end{aligned}$$

With an environment input u_{env} added to the motor torques u, the error dynamics become:

$$\begin{aligned} &D(q)\ddot{\tilde{x}}_1 + C(q,\dot{q})\dot{\tilde{x}}_1 + C\left(q,\dot{\hat{x}}_1\right)\dot{\tilde{x}}_1 \qquad (15)\\ &\quad = -K_p\tilde{x}_1 - k_vD(q)\dot{\tilde{x}}_1 + u_{env}\ , \end{aligned}$$

which have an equilibrium point that acts again like a stretched spring:

$$\bar{x}_1 = {K_p}^{-1}u_{env}\ . \tag{16}$$

Theorem 1 *[1] Assume that $|\dot{q}(t)| \le M$ for any $t \ge 0$. If $k_c > 0$ is such that $\|C(q,\dot{q})\| \le k_c\|\dot{q}\|$ and $k_v > \frac{k_cM}{\underline{\lambda}(D)}$, then the equilibrium point, $[\tilde{x}_1,\dot{\tilde{x}}_1] = [0,0]$, is asymptotically stable, and a region of attraction is given by*

$$S = \left\{ x\epsilon R^{2N} : \|x\| < \sqrt{\left(\frac{\underline{\lambda}(H)}{\bar{\lambda}(H)}\right)\left(\frac{\underline{\lambda}(D)\,k_v}{k_c} - M\right)} \right\} \tag{17}$$

where $H = diag[K_p, D(q)]$, and $\underline{\lambda}$ and $\bar{\lambda}$ denote the minimum and maximum singular value, respectively.

It is easy to show [9] that a constant environment input u_{env} causes the equilibrium point to shift from $[\tilde{x}_1,\dot{\tilde{x}}_1] = [0,0]$ to $[\tilde{x}_1,\dot{\tilde{x}}_1] = [{K_p}^{-1}u_{env},0]$, and has a shifted region of attraction as in (17).

5 Experimental Results

Rigid body control was performed on the six-degree-of-freedom UBC maglev wrist [6]. The wrist levitates a rigid *flotor* through currents applied to coils situated between strong magnets. Position and orientation of the flotor is measured via light emitted from diodes on the flotor directed onto position sensing devices. The absence of contact between the flotor and its base through anything other than lightweight flexible umbilical cables has the flotor well described by a rigid body model.

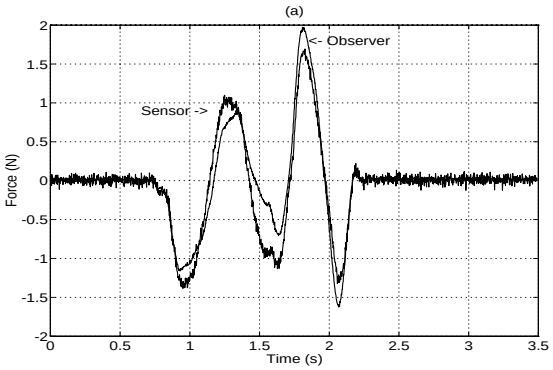

Figure 4: Sensor and Estimated Force (x-component).

5.1 Inertial Parameter Identification

The observer algorithms presented require an accurate model of the rigid body inertial parameters. The recursive least-squares parameter identification procedure outlined in [8] was used to determine the mass properties of the flotor. The rigid body dynamics were written in the "linear-in-paramters" form [8]:

$$\begin{bmatrix} f \\ \tau \end{bmatrix} = \begin{bmatrix} a & [\dot{\omega}\times] + [\omega\times]^2 & 0 \\ 0 & [-a\times] & [\dot{\omega}\bullet] + [\omega\times][\omega\bullet] \end{bmatrix}\theta$$

$$\theta = [m, mc_1, mc_2, mc_3, J_{11}, J_{12}, J_{13}, J_{22}, J_{23}, J_{33}]^T$$

where a is the body linear acceleration with gravity offset removed, f and τ are the applied forces and torques, $[c_1c_2c_3]^T$ is the center of mass, and

$$[\omega\bullet] = \begin{bmatrix} \omega_1 & \omega_2 & \omega_3 & 0 & 0 & 0 \\ 0 & \omega_1 & 0 & \omega_2 & \omega_3 & 0 \\ 0 & 0 & \omega_1 & 0 & \omega_2 & \omega_3 \end{bmatrix} \tag{18}$$

$$[\omega\times] = \begin{bmatrix} 0 & -\omega_3 & \omega_2 \\ \omega_3 & 0 & -\omega_1 \\ -\omega_2 & \omega_1 & 0 \end{bmatrix}. \tag{19}$$

All variables are expressed with respect to a defined body frame, and J_{ij} are the entries of the inertia matrix about the flotor frame origin. Numerical differentiation and low-pass filtering were used to obtain the required data matrices, while f and τ were determined from flotor coil currents [9]. The results of the recursive least-squares identification are shown in Tables 1 and 2.

5.2 Force Torque Estimation

A JR3 force/torque sensor was mounted on the wrist flotor to allow for comparison to the observer based force estimation. The inertial parameters were then identified. Results shown in Figures 4 and 5 confirm the effectiveness of the force torque estimation technique in a practical setting (in this case and in the next subsection only x components of each time varying vector are plotted for brevity). Further details on the experimental setup and experiment parameters can be found in [9].

Table 1: Results of the Identification for Flotor Alone: Inertial parameters of the wrist flotor are difficult to determine without identification

	Mass (kg)	Center (cm)	Inertia Matrix (gm^2)		
Estimated Values	0.604	-0.04	0.781	0.003	-0.007
		0.03	0.003	0.819	-0.005
		-0.11	-0.007	-0.005	1.038

Table 2: Results of the Identification for Flotor with Iron Block Mounted: An iron block with known inertial properties was mounted on the flotor. Results show a change in the inertial parameter estimates from those shown in Figure 5.1. The bottom entries show the change calculated from the known inertia of the block and it's position on the flotor.

	Mass (kg)	Center (cm)	Inertia Matrix (gm^2)		
Estimated Values	1.133	0.11	4.145	0.105	-0.050
		-0.00	0.105	4.250	0.089
		3.70	-0.050	0.089	1.115
Estimated Change	0.5258	0.15	3.364	0.109	-0.043
		0.04	0.109	3.431	-0.130
		3.81	-0.043	-0.130	0.077
Calculated Change	0.530	0.00	2.930	0.000	0.000
		0.00	0.000	2.919	0.000
		3.33	0.000	0.000	0.063

5.3 Output - Corrected Observer

Figure 6 illustrates considerable noise reduction without significant degradation of velocity estimates. First, the wrist flotor was controlled in PID mode, with no sensor attached. At time $t = 0.4s$, torque was applied to the flotor by shaking it by hand. Contact was lost at $t = 1.7s$. Figure 6.a shows the estimated environment torque. In Figure 6.b, serious discrepancies are noted between velocity obtained by differentiation and the velocity measured using an uncorrected observer. Comparison of the corrected velocity observer output (Figure 6.c) to that of the velocity obtained through numerical differentiation demonstrates that the corrected velocity observer tracks the true velocity. It should be noted that offsets in the observed velocity, clearly visible from $t = 0.0s$ to $t = 0.4s$ and $t > 2.0s$, are removed effectively. As expected, correcting the velocity observer adds noise to the velocity estimate, but the noise levels can be seen to be less than when differentiation is used.

5.4 Input Corrected Observer

Two observers were implemented, one with faster time constants to estimate the environment forces, the other to estimate the body velocity. The estimated environment forces were added to the velocity observer input as shown in Figure 3. As can be seen in Figure 7, in the presence of environment forces, the uncorected observer produces estimates that differ substantially

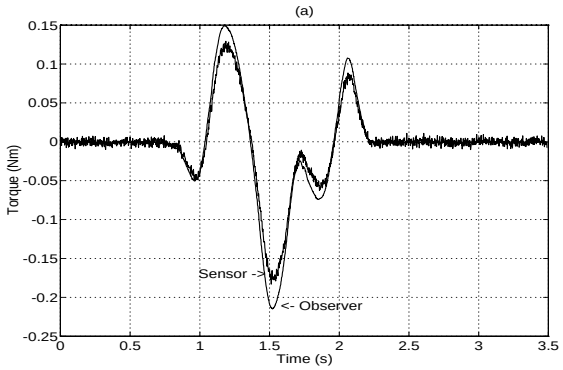

Figure 5: Sensor and Estimated Torque (x-axis)

from those obtained by direct differentiation (compare Figure 7.b to Figure 7.c), while only a small error due to the band-limited force estimate can be seen for the input corrected observer.

6 Conclusions

The correct execution of tasks by manipulators often require knowledge of environment forces and manipulator velocities. It was shown, analytically and experimentally, that if an accurate dynamic model of a robot is available, accurate environment force and manipulator velocity estimates can be obtained using model-based observers.

Therefore, the robot velocities and environemnt forces and torques can be obtained without the use of expensive sensors or noisy differentiation of signals. The technique presented is particularly well-suited to direct-drive mechanisms that can be accurately modelled and that can apply accurate forces.

Applications to teleoperation, assembly and vibration isolation using a maglev wrist will be pursued.

References

[1] S. Nicosia and P. Tomei, "Robot control by using only joint position measurements," *IEEE Trans. Automat. Cont.*, pp. 1058–1061, Septmeber 1990.

[2] W.-H. Zhu, H.-T. Chen and Z.-J. Zhang, "A Variable Structure Rohbot Control Algorithm with an Observ er," *IEEE Trans. Robotics Automat.*, vol. 8, August 1992.

[3] R.L. Hollis, S.E. Salcudean, and P.A. Allan, "A Six Degree-of-Freedom Magnetically Levitated Variable Compliance Fine Motion Wrist: Design, Modelling and Control," *IEEE Transactions on Robotics and Automation*, vol. 7, pp. 320–332, June 1991.

[4] S.-R. Oh, R.L. Hollis, and S.E. Salcudean, "Precision Assembly with A Magnetically Levitated Wrist," in *Proceedings of the IEEE International Conference on Robotics and Automation*, (Atlanta, USA), pp. 127–134, May 2-6, 1993.

[5] S.E. Salcudean, H. Davis, C.T. Chen, D.E. Goertz, and B. Tryggvason, "Coarse-Fine Residual Gravity Cancellation System with Magnetic Levitation,"

in *Proceedings of the IEEE International Conference on Robotics and Automation*, (Nice, France), pp. 1641–1647, May 10-15, 1992.

[6] S.E. Salcudean, N.M. Wong, and R.L. Hollis, "A Force-Reflecting Teleoperation System with Magnetically Levitated Master and Wrist," in *Proceedings of the IEEE International Conference on Robotics and Automation*, (Nice, France), pp. 1420–1426, May 10-15, 1992.

[7] S.E. Salcudean, "A Globally Convergent Angular Velocity Observer for Rigid Body Motion," *IEEE Transactions on Automatic Control*, vol. 36, pp. 1493–1497, December 1991.

[8] C.H. An, C.G. Atkeson, and J.M. Hollerbach, *Model-Based Control of a Robot Manipulator*. Cambridge, MA: MIT Press, 1988.

[9] P.J. Hacksel, "Observer based velocity and environment force estimation for rigid body control," Master's thesis, University of British Columbia, October 1993.

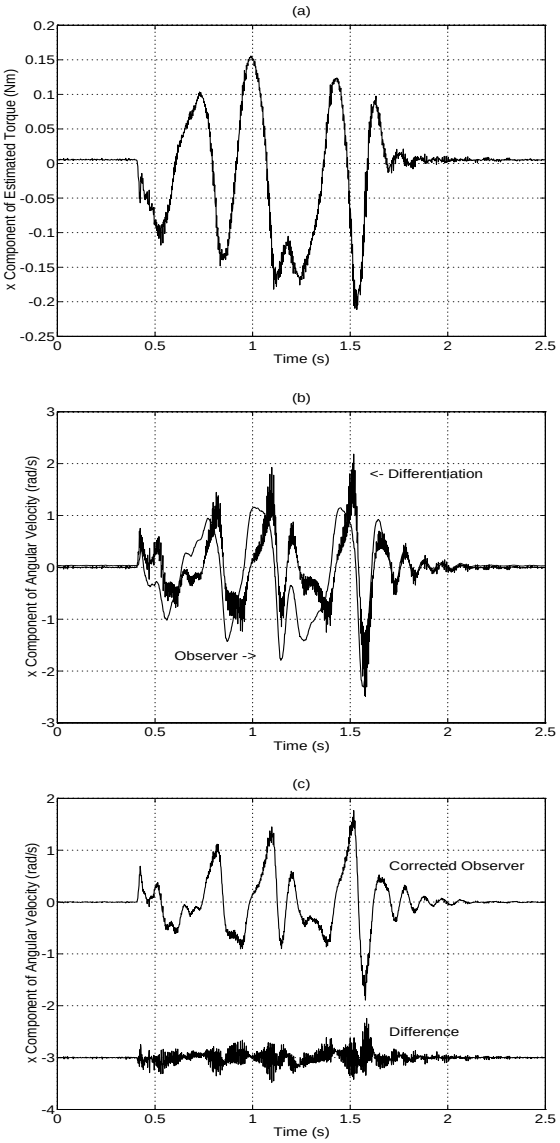

Figure 6: Output Corrected Velocity Observer Experiment: (a) Observed Torque in Input Corrected Velocity Observer Experiment, (b) Velocity Observed with Uncorrected Observer vs that Obtained by Numerical Differentiation, (c) Velocity Observed With Corrected Observer and Difference From Numerical Differentiation: The true angular velocity is found by numerically differentiating the quarternion parameter and calculating $\omega = [\beta_o I - (\beta\times)]\dot{\beta}$. The observer estimated velocity is seen to deviate from the true velocity when torque is applied. The corrected observer closely follows the true velocity in spite of the existence of environment torques and with a significant reduction in the noise level. The difference between the corrected observer velocity and the numerically differentiated velocity is plotted at the bottom of the third figure (offset by 3 rad/sec) and consists mostly of noise.

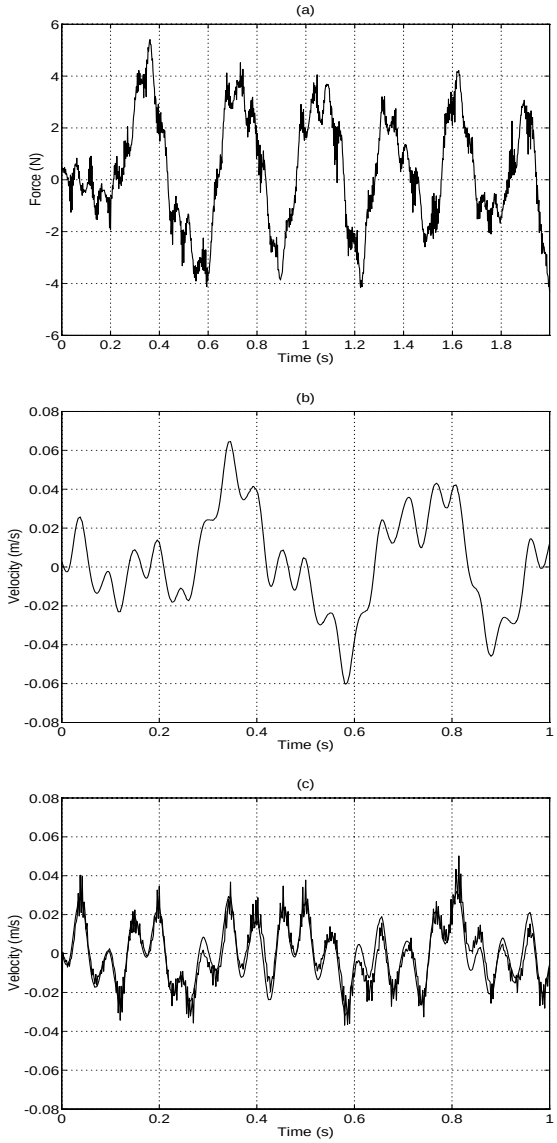

Figure 7: Input Corrected Velocity Observer Experiment: (a) Observed Force, (b) Velocity Observed With Uncorrected Observer, (c) Velocity Observed with Corrected Observer vs that Obtained by Numerical Differentiation: The uncorrected observer velocity is again seen to be dramatically affected by the environment force. Close correspondence of corrected observer velocity and true velocity is seen. The filtering action of the second observer leads to less noisy results.